Property of RF Capacitive Discharge Containing Oxygen Negative Ions

H. Amemiya, N. Yasuda* and M. Endo*
The Institute of Physical and Chemical Research (RIKEN)
Hirosawa 2-1, Wako, Saitama-Pref. 351-01, JAPAN
*Chuo University, Faculty of Engineering
Bunkyo-ku, Kasuga, Tokyo 110, JAPAN

The parallel-plate RF discharge has been investigated in oxygen between 10^{-3} and 1 Torr. The plasma contains negative ions, and the negative ion density becomes maximum at optimum RF power and pressure. The electron energy distribution f(E) deviates from the Maxwellian energy distribution. The low energy part is extremely deficient, which means that the process of negative ion formation by dissociative attachment is occurring. A higher energy group appears due to electrons accelerated from the cathode sheath. The variation of negative ion density vs RF power has been compared with that of calculation based on the treatment by the electron temperature. The result suggests that complete agreement would be obtained only by considering actual non-Maxwellian energy distributions.

1. Introduction

The oxygen plasma often appears in the plasma processing such as oxidation, ashing, generation of ozone and radicals, etc. It is also important in obtaining a negative ion beam. In a former work on the RF discharge in oxygen, the generation of ozone and negative ions was discussed [1]. A later work was directed to the electron energy distribution f(E), but little discussion was made on negative ions [2]. In our previous work of oxygen RF discharge [3] with parallel-plate floated electrodes, the electron energy distribution f(E) and the negative ion density were measured, but the relation between them was not totally clarified. Recently, the RF plasma in oxygen has been investigated both experimentally and theoretically in parallel-plate and cavity configurations [4] by measuring the density of negative ions by the photodetachment technique using the microwave cavity method. A good comparison with modelling is shown, although f(E) is assumed to be Maxwellian. In many cases, the treatment by the electron temperature is not appropriate in the plasma processing.

The purpose of the present work is to extend our previous work [3] to clarify the role of f(E). Nitrogen RF discharges without negative ions are measured for comparison. The negative ion density is also measured by the photodetachment technique using YAG lasers with the probe detection. This method can be more generally applied to any configurations of set-up, when the determination of the absolute value is made with the aid of the probe second derivative.

2. Experimental Apparatus

Figure 1 shows a schematic diagram of the capacitive RF discharge. The discharge is made between parallel-plate electrodes E with a spacing of 2.5cm and a diameter of

8cm set in a cross-type Pyrex glass tube T. RF power of 13.56MHz is sent from a RF oscillator RF through a balanced-type matching M. The electrodes are symmetrically floated from the ground and mounted inside a magnetic multipole cusp MP to confine the plasma. After the tube was evacuated by a diffusion pump DP and a rotary pump RP below 10^{-6} Torr, O_2 or N_2 was made to flow through a mass-flow controller at a desired pressure between 1 mTorr and 1 Torr. A disk probe P was inserted between the electrodes to obtain the probe characteristics i_p. The energy distribution f(E) was derived from the probe second derivative i_p'' by the so-called Druyvesteyn method.

In order to measure i_p without distortion by the RF field, the apparatus was mounted in an electromagnetic double-shield chamber, as schematically shown in Fig.2, and AC power was supplied through a band-pass filter BPF for 50Hz. Tuned LC filters F_t were inserted into the probe circuit. The power supply for the probe bias V_p, XY recorder and lock-in amplifier PSD for the measurement of i_p'' were placed outside the chamber. Signal was passed through band-eliminator filters BEF for 13.56MHz. The second derivative i_p'' was measured by the beat technique by superimposing two sine waves from a crystal oscillator OSC on V_p via a transformer T_c and picking up the beat wave component from another transformer T_p.

In order to obtain the optogalvanic (OG) signal due to the photodetachment of O^- and O_2^-, the plasma was irradiated by cw YAG of 1.06μm and Q-switched pulsed YAG lasers of 1.06μm and 532 nm. The laser beam was focused by a lens L near the probe P. The OG signal picked up by the probe was measured phase-sensitively by a lock-in amplifier PSD through double chopping by choppers C (344Hz) and C_s (23s) in the cw mode. In the pulsed mode, it was measured by a digital storage oscilloscope DSO and the averaged waveform for multi-shots was recorded. Light from a halogen lamp is passed through the plasma and the transmitted light is measured by a monochromator MC through an optical fiber OF to detect dust.

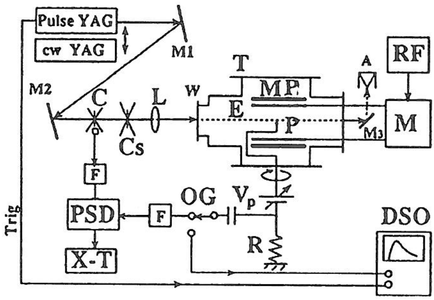

Fig. 1

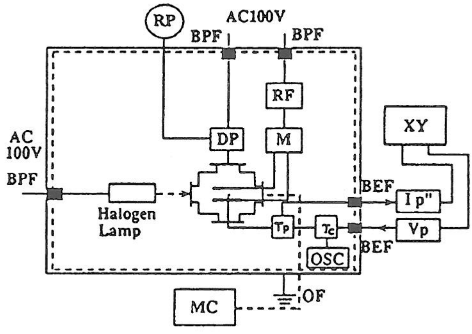

Fig. 2

3. Experimental Results

Figures 2 shows an example of f(E), f_{exp}, in O_2 compared with models given by eq.(1), which was obtained on the assumption with only elastic collisions [5]. I.e.,

$$f(E) = \frac{m\Gamma(\frac{5}{2m})^{3/2}\sqrt{E}}{\Gamma(\frac{3}{2m})^{5/2}E_m^{3/2}} \exp\left\{-\frac{m\Gamma(\frac{5}{2m})^{m}E^{m}}{\Gamma(\frac{3}{2m})^{m}E_m^{m}}\right\}, \qquad (1)$$

where Γ(m) is the complete Gamma function, m=1, 2 and 3 correspond to Maxwellian f_M, Druyvesteyn f_D and Rutscher's type f_4 [5], respectively, E_m is the average energy and f(E) is normalized as $\int_0^\infty f(E)dE=1$.

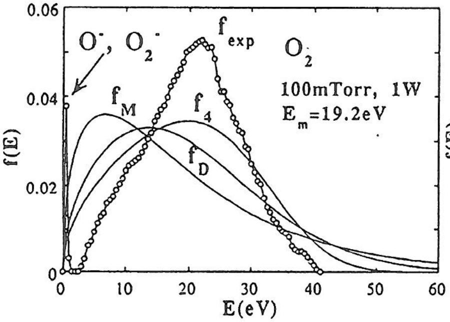

Fig. 3

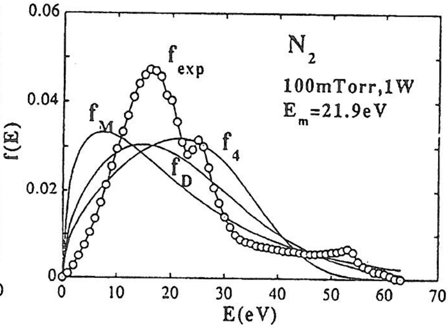

Fig. 4

Figure 3 shows a typical f(E) in O_2. The population of the low energy part below 10eV is small, which may be due to the loss by negative ion formation through dissociative attachment, the cross-section of which lies at about 6.8eV [6]. The middle energy part corresponds to thermal electrons and the higher energy part above 30eV corresponds to superthermal ones. It has been confirmed by rotating the probe that the high energy group (sometimes a bump) comes from the cathode sheath. The relative population of the higher energy group increases with the RF power P_f and decreasing pressure p. A sharp peak near E=0 corresponds to oxygen negative ions, O^- and O_2^-.

Figure 4 shows a typical f(E) in N_2, which consists of thermal electrons peaking at energies of about 17eV and a high energy group above 40eV. No such a sharp peak due to negative ions near E=0 is seen. The high energy tail or bump becomes more remarkable with increase of P_f and decrease in p. The effect of the cathode sheath to sustain the discharge by primary electrons is clear both in O_2 and N_2.

The procedure of obtaining the plasma parameters is as follows. First, the negative ion temperature T_- has been determined from the i_p''-peak near E=0 as $1/kT_- = dLn(i_p'')/dV_p$ to be 0.2 to 0.6 eV. T_- increases gradually with P_f and decreases with p. The electron density N_e is obtained form the electron saturation current in the usual manner. The effective negative ion density N_{-eff} has been determined from the peak heights of i_p'' for electron and negative ions, i_{pe}'' and i_{p-}'', T_- and N_e from eq.(2) by defining the effective negative ion mass M_{-eff} and the mean energy E_m as

$$N_{-eff} = N_e\sqrt{\frac{M_{-eff}}{m_e}}\,\frac{T_-^{3/2}}{(2E_m/3)^{3/2}}\,\frac{i_{p-}''}{i_{pe}''}\ ;\quad M_{-eff}^{-1} = \sum_j \frac{N_{-j}}{M_{-j}}\ , \qquad (2)$$

where m_e is the electron mass, N_{-j} is the density of j-th negative ion species and E_m was calculated from $E_m = \int_0^\infty Ef(E)dE$.

Figures 5 shows the output of PSD in the case of cw laser after chopping the laser beam by the slow chopper C_s (cf. Fig.1). The OG signal intensity is obtained from the amplitude. The irregularity of the base line of PSD is thus avoided.

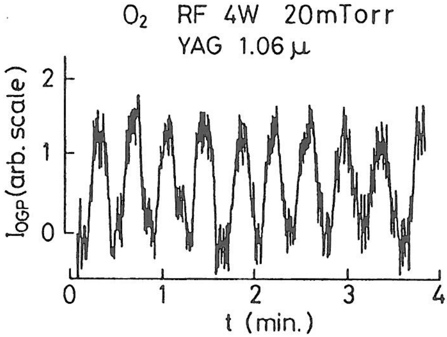

Fig. 5

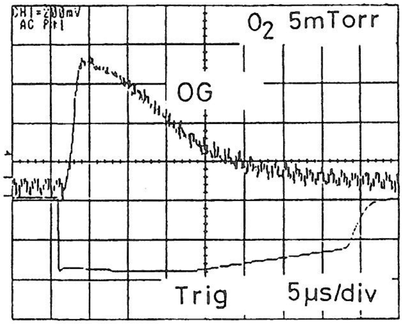

Fig. 6

Figure 6 shows a waveform of OG signal by the pulsed laser averaged by 16 shots. The negative ion density has been estimated from the amplitude I_{OG} or the area of the waveform Q_{OG} as

$$I_{OG} = \frac{eP_L L}{h\nu} \sum_{j=1}^{3} N_{-j}\, \sigma_j(\nu)\ ; \qquad Q_{OG} = \frac{eW_L L}{h\nu} \sum_{j=1}^{3} N_{-j}\, \sigma_j(\nu)\ , \qquad (3)$$

where ν is the laser frequency, P_L and W_L are the laser power and energy, $\sigma_j(\nu)$ is the photodetachment cross-section of negative ions of j-th species at ν, and L is the interaction length between the laser and the plasma. L should be estimated from a comparison of N_- by probe and OG methods.

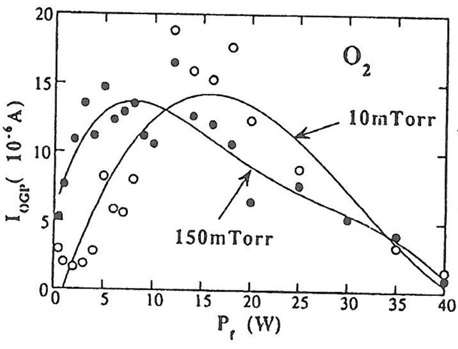

Fig. 7

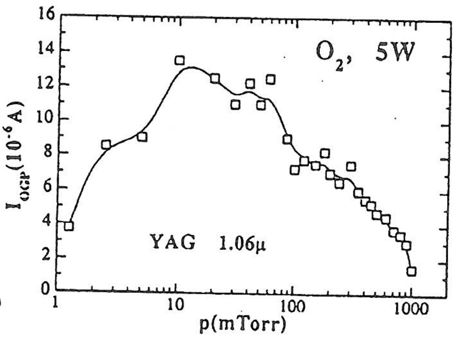

Fig. 8

Figures 7 and 8 show power and pressure dependences of the OG signal intensity I_{OGP} determined from the peak height of the OG waveform. I_{OGP}, or N_-, increases with P_f and reaches a maximum at about P_f =7-20W and N_- becomes maximum at 10-50 mTorr. Photodetachment signals by the pulsed lasers of 1.06μm and 532nm has indicated that negative ions O^- and O_2^- exist.

4. Discussion

The appearance of non-thermal electrons especially at low pressures and high RF powers suggests the effect of cathode fall on the maintenance of the RF discharge. When P_f is increased, the average electron energy E_m increased and this caused an increase in the potential depth of the sheath. Therefore, the effect of primary electrons on the plasma production is enhanced. This may be related to the so-called γ-regime [7,8]. In our discharges, however, the difference of discharge mode, or the brightness of the glow between two regimes was not distinct. The change in the average energy of thermal electrons at the transition as observed in Ar [8] was not remarkable.

Rate equations of oxygen discharges have been calculated for the present RF discharge. About 70 reactions as in ozone generation [9] has been included. Considered species are O, $O(^1D)$, $O_2(\Delta_g)$, O_2, O_3, O^-, O_2^-, O_3^-, electrons and positive ions, O^+ and O_2^+ with their densities defined as N_{01}, N_D, N_{02}, N_g, N_{03}, N_1, N_2, N_3, N_e, N_{+1} and N_{+2}, respectively. As the loss mechanism, the diffusion and recombinations are considered. The charge balance is expressed as

$$N_+ = \sum_{j=1}^{2} N_{+j} = N_e + \sum_{j=1}^{3} N_{-j} . \qquad (4)$$

It has been found by checking the numerical result that the gain and loss of ion species are mainly given by the following reactions.

	Gain	Loss
O^-	$O_2 + e \rightarrow O + O^-$ (R2)	$O^- + O_2^+ \rightarrow O + O_2$ (R6)
		$O^- + O_2 \rightarrow O_3 + e$ (R26b)
		$O^- + O_2^+ + M \rightarrow O_3 + M$ (R30)
		$O^- + O_2 + M \rightarrow O_3^- + M$ (R52)
O_2^-	$O_2(\Delta g) + O^- \rightarrow O_2^- + O$ (R18b)	$O_2^- + O_2^+ + M \rightarrow 2O_2 + M$ (R46a)
	$O_2 + e + M \rightarrow O_2^- + M$ (R36a)	$O_2^- + O_2^+ \rightarrow 2O_2$ (R46b)
		$O_2^- + O_2^+ \rightarrow O_2 + 2O$ (R46c)
		$O_2^- + O_2(\Delta g) \rightarrow 2O_2 + e$ (R50)
O_3^-	$O^- + O_2 + M \rightarrow O_3^- + M$ (R52)	$O_2^+ + O_3^- \rightarrow O_2 + O_3$ (R48a)
		$O_2^+ + O_3^- \rightarrow 2O + O_2$ (R48b)
		$O_3^- + M \rightarrow O_3 + e + M$ (R61)
O^+	$O_2 + e \rightarrow O^+ + O + 2e$ (R25)	$O^+ + O_2 \rightarrow O_2^+ + 2O$ (R56)
O_2^+	$O_2 + e \rightarrow O_2^+ + 2e$ (R1)	$O_2^+ + O_2 + O_2 \rightarrow O_4^+ + O_2$ (R67)
	$O^+ + O_2 \rightarrow O_2^+ + 2O$ (R56)	

where the same number is attached to the reactions as given in [9]. Main generation mechanism for negative ions in the glow region, where E/N=50Td, T_e=3eV, $N_e=10^8$-10^9, are the generation of O^- by dissociative attachment , (2) O_2^- by the charge transfer from O^-. The density of O_3^- is much smaller than those of O^- and O_2^-. Dominant positive ions are O_2^+: N_{+1} is found to be much smaller than N_{+2}.

Figure 9 shows the flow chart of calculation. Calculation of the density of neutral species has been performed first followed by that of the density of ion species based on neutral species. Calculation is iterated by varying the diffusion losses for negative and positive ions until the charge neutrality (4) is satisfied.

Figure 10 shows an example of the calculated result on negative ion densities vs N_e. From experiment it has been found that N_e is nearly proportional to the RF power P_f. The negative ion densities show no peak or a more gentle peak vs N_e than in the experiment. One of the reasons for discrepancy is considered to be due to the non-Maxwellian energy distribution, which would cause a reduction in N_- at higher P_f. Such an effect has not been taken into account in the calculation. Another reason may be in the generation of dusty particles. The transmitted light intensity between 400 and 800nm of a halogen lump has indicated absorption by RF plasma [10]. Since the dust density increases with P_f, N_- could be decreased with it.

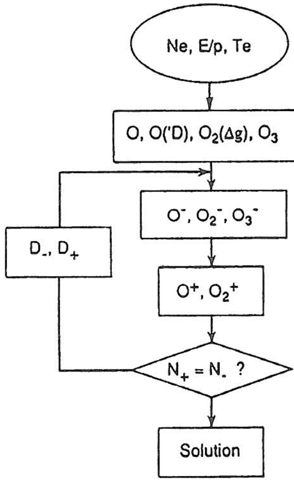

Fig. 9

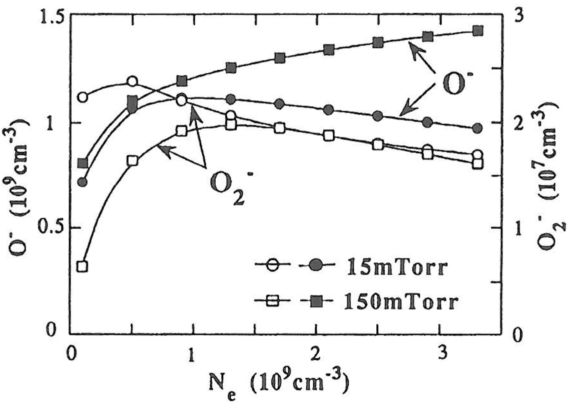

Fig. 10

5. Conclusion

From the experiment on the parallel-plate RF discharge in oxygen, it has been found that the negative ion density becomes a maximum at an optimum RF power and a pressure. The measured f(E) indicates that the discharge is sustained partly by superthermal electrons from the cathode sheath as in the case of DC discharge. The result of OG data has been compared with a modelling but only rough agreement has been obtained since f(E) is strongly deviated from the Maxwellian energy distribution.

This work is supported by Grant-in-Aid from the Japan Ministry of Education, Science and Culture. We thank Mr. Y.Ogata, Musashi Institute of Technology, and Ms. K.Ogawa, Chuo University, for their support in the experiment.

References

[1] A.T.Bell, Industr. Eng. Chem. Fundam. **10**, 273 (1971).
[2] H.Sabadil,S.Klagge & M.Kammeyer, Plasma Chem.Plasma Proc. **8**, 425 (1988).
[3] H.Amemiya, N.Yasuda & M.Endo, Plasma Chem.Plasma Proc.**14**, 209 (1994).
[4] E.Stoffels, W.W.Stoffels, D.Vender, et al., Phys.Rev.E **51**, 2425 (1995).
[5] T.Ruzicka, A.Rutscher and S.Pfau, Ann. Physik **24**, 124 (1970).
[6] Y.Itikawa, A.Ichimura, K.Onda, et al., J.Phys.Chem.Ref.Data, **18**, 23 (1989).
[7] Y.P.Raizer, Gas Discharge Physics, Springer Verlag, p. 388, 1987.
[8] V.A.Godyak and R.B.Piejk, Plasma Source Sci.Technol.**1**, 36 (1992).
[9] B.Eliasson and U.Kogelschatz, Basic Data for Modelling of Electrical Discharges in Gases: Oxygen, Brown Boveri Konzernforschung 1986.
[10] H.Amemiya, K.Ogawa, N.Yasuda & M.Endo, Proc. 2nd Asia-Pacific Conf. Plasma Sci. Technol., Tajeon, Korea, 1994, pp.209-212.